

The *ef* loop of cyt *b* is a conspicuous barrier for the movement of the Fe-S subunit of the *bc*₁ complex during Q_o site catalysis

E Darrouzet¹ and F Daldal²

¹*Service de Biochimie Post-génomique et Toxicologie Nucléaire, DIEP, DSV, CEA VALRHO, 30207 Bagnols sur Cèze, France email: DARROUZET@dsvsud.cea.fr*

²*Department of Biology, Plant Science Institute, University of Pennsylvania, Philadelphia, PA 19104, USA email: fdaldal@sas.upenn.edu*

Keywords : cytochrome *bc*₁ complex, Rieske FeS subunit, large- scale domain movement, Q_o site catalysis, *Rhodobacter capsulatus*

Introduction

The *bc*₁ complex is a quasi-ubiquitous multisubunit protein that is an important part of both respiratory and photosynthetic electron transport chains (1). This enzyme conveys electrons from ubihydroquinone (QH₂) to a *c*-type cytochrome (cyt) in a manner coupled to proton translocation across the membrane. The electrochemical gradient thus generated is subsequently used for ATP synthesis. The mechanism of function of this enzyme is best described by the Q-cycle model (2,3), that features as a critical step the bifurcation of electrons derived from the oxidation of QH₂ at the QH₂ oxidation (Q_o) site to two distinct routes. One of these electrons follows the high potential chain constituted of the [2Fe2S] cluster carried by the Fe-S subunit and *c*₁ heme on the cyt *c*₁ subunit. The other electron is conveyed to the low potential chain constituted by 2 *b*-type hemes (*b*_L and *b*_H), and reduces an ubiquinone (Q) (or a ubisemiquinone (QS) radical) in a second catalytic site (Q_i site) located across the membrane.

In recent years, major progress has been accomplished upon the resolution of the 3D structure of the *bc*₁ complex (4-7). Comparison of various structures revealed that the cluster domain of the Fe-S subunit occupies different positions in the enzyme complex (4-7). Subsequent biochemical, biophysical and genetic studies (8-16) have now established firmly that the Fe-S subunit acts as an unprecedented electron shuttle via a large-scale domain movement between the Q_o site of the enzyme and its cyt *c*₁ subunit. Mutations located in the linker domain of the Fe-S subunit that acts as a hinge during the domain movement interfere with the mobility of the cluster domain of this subunit (8,9, 12,14-17). Especially, mutants that contained Ala insertions in the hinge exhibited slower movement and enabled for the first time to unveil kinetically the electron transfer associated with it (14). However, little is known about whether this movement is controlled or not, and if so, what are the regions of the *bc*₁ complex implicated in this control. In this work, we show that a mutant with a single Ala insertion in the hinge of the Fe-S subunit can regain full function via a second mutation located in the *ef* loop of cyt *b*. The data obtained indicate that the *ef* loop region of cyt *b* constitutes an obvious physical barrier that needs to be crossed during the movement of the Fe-S subunit from the Q_o site to the cyt *c*₁ in order to sustain the catalytic turnover of the *bc*₁ complex.

Materials and methods

Bacterial strains were grown as in (15). All biochemical and biophysical techniques are also described in (15) except that a dual wavelength spectrophotometer, instead of a single wavelength spectrophotometer (Biomedical Instrumentation Group, University of Pennsylvania, Philadelphia, PA. USA) was used for some of the time-resolved, light activated cyt *c* re-reduction or cyt *b* reduction kinetics.

Results

The slower phototrophic (Ps) growth of the +1Ala mutant of *R. capsulatus*, due to its impaired *bc*₁ complex (14), allowed us to isolate its faster growing derivatives. Analyses of these isolates indicated that they contained a second mutation that substituted the Leu at position 286 of the *ef* loop of cyt *b* by a Phe. The L286F mutation being the molecular basis of the improved Ps growth of the +1Ala mutant was established by exchanging the 920 bp *Xma*1-*Sfu*1 fragment carrying it with its wild type counterpart in the +1Ala mutant background. In addition, this fragment was also introduced into a wild type background to obtain a single mutant that carried only the L286F mutation. All mutants assembled the Fe-S subunit in the complex as indicated by SDS-PAGE gels and western blot analyses (data not shown), although a slight sub-stoichiometry of the Fe-S subunit could be seen whenever the L286F mutation was present. EPR spectra revealed that the interactions of the [2Fe2S] cluster with Q or the inhibitor stigmatellin were native-like in all strains as indicated by the usual 1.800 and 1.783 *g*_x signals (14-15) (data not shown).

The steady-state activity of mutant *bc*₁ complexes indicated that L286F mutation decreased the ability of the enzyme to reduce cyt *c*. This was possibly due to the sub-stoichiometry of the Fe-S subunit and the increased sensitivity of the *bc*₁ complex to detergent, as previously observed with for example the hinge deletion mutants that have assembly defects (15). Next, the effect of the L286F mutation on the [2Fe2S] cluster *E*_m was sought, and the *E*_{m7} values of the [2Fe-2S] cluster in the mutants indicated that the L286F mutation decreased in all cases the *E*_{m7} values by about 50 mV. Various properties of these mutants are summarized in **Table 1**.

A more detailed study of the *bc*₁ complex function in the mutants was undertaken by analyzing their single turnover kinetics (14). First, the measurements were performed at a *E*_h of 100 mV where the *Q*_{pool} contains both Q and QH₂, and the [2Fe2S] cluster is reduced. After a flash of light to activate the reaction center and oxidize the *c*-type cyt, the cyt *c* re-reduction kinetics were followed at 550-540 nm, and the cyt *b* reduction kinetics at 560-570 nm in the presence of 5 μM antimycin A. The results shown in **Fig. 1** revealed similar effects on the cyt *b* and *c* kinetics. The L286F mutation alone impeded the function (**Fig. 1**, compare panels A and B), and the relative activity of the +1Ala/L286F revertant was not higher than that of the +1Ala alone when the visible portions of the kinetics (which reflect events later than the initial QH₂ oxidation at the *Q*_o site) were compared. However, it was clear that the slow electron transfer phase observable in presence of myxothiazol in the +1Ala mutant (14) was no longer discernable in the case of the +1Ala/L286F revertant (**Fig. 1**, compare panels C and D). The data suggested that this mutant had recovered the fast movement of its Fe-S subunit, which was consistent with its better Ps growth ability. The cyt *b* kinetics measurements were also repeated at an *E*_h value of 400 mV at which the [2Fe2S] cluster is oxidized.

The +1Ala and +1Ala/L286F exhibited wild-type like cyt *b* reduction kinetics, indicating that the QH₂ oxidation at the Q_o site was not affected in these mutants even though the electron transfer from the [2Fe-2S] cluster to cyt *c*₁ was slower (**Table 1**). Indeed, this activity was fully inhibited by myxothiazol (not shown) and was not discernable in a mutant with a defective Q_o site catalysis such as Y147A (19).

Table 1: Characteristics of the +1Ala/L286F revertant and its derivatives

	Ps phenotype ^a	Assembly ^b (%)		E _{m7} [2Fe-2S] (mV) ^c	Steady-state Activity (%) ^d	Electron transfer QH ₂ → cyt <i>c</i> (%) ^e	Electron transfer QH ₂ → cyt <i>b</i> (%) ^f	
		Fe-S subunit	[2Fe-2S]				100 mV	400 mV
WT	Ps ⁺	100	100	310	100	100	100	100
L286F	Ps ⁺	60	40	260	20	60	35	45
+1Ala	Ps ^{slow}	105	140	370	120	35	25	125
+1Ala/L286F	Ps ⁺	80	100	320	60	35	40	115

^aPs⁺, Ps^{slow} and Ps⁻ refer to phototrophic growth ability of various mutants.

^bAssembly Fe-S subunit and [2Fe-2S] cluster refer to the stoichiometry of the Fe-S subunit in respect to the cyt *c*₁ or cyt *b* subunits as determined by scanning of SDS-PAGE gels and immunoblots, and the relative amounts of the [2Fe-2S] cluster in comparison to the wild-type, as determined by the amplitude of the EPR *g_y* signal, respectively. All values are expressed as a percentage of the wild-type (15).

^cThe E_{m7} values were obtained after fitting the amplitude of the EPR *g_y* signal during potentiometric dark titration of the [2Fe-2S] cluster (15).

^dSteady-state refers to the DBH₂: cyt *c* reductase activity expressed as a percentage of the wild-type activity which was approximately 3 μmol of cyt *c* reduced min⁻¹ mg of membrane protein⁻¹ (18).

^eQH₂ to cyt *c* electron transfer rates were determined at 100 mV by recording cyt *c* re-reduction kinetics at 550-540 nm and fitting them to a single exponential equation (15). They are presented as a percentage of that of the wild-type which was approximately 300 s⁻¹.

^fQH₂ to cyt *b* electron transfer rates were determined either at an E_h of 100 or 400 mV by recording cyt *b* reduction kinetics in presence of 5 μM antimycin A at 560-570 nm, and fitting them to a single exponential equation (15). They are expressed as a percentage of that of the wild-type which were approximately 500 s⁻¹ and 60 s⁻¹ at 100 and 400 mV, respectively.

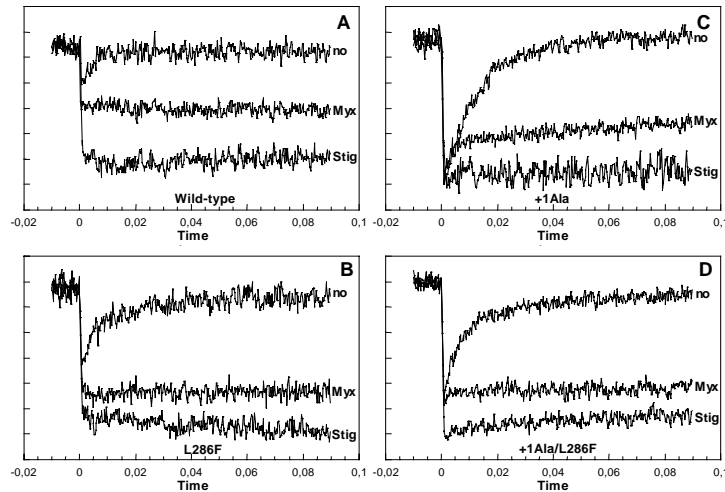


Figure 1. Cyt *c* re-reduction kinetics in the presence of myxothiazol or stigmatellin in various mutants. Cyt *c* re-reduction kinetics were triggered by flash-activation of the photochemical reaction center and recorded at 550 - 540 nm using chromatophore membranes poised at 100 mV as described in (15). In each case, the traces obtained with no inhibitor (no), or in the presence of myxothiazol (Myx) (no QH₂ oxidation), or in the presence of stigmatellin (Stig) (no electron transfer to cyt *c*₁ heme) are shown. Panels A, B, C and D correspond to the wild type, L286F, +1Ala and +1Ala/L286F mutant strains, respectively.

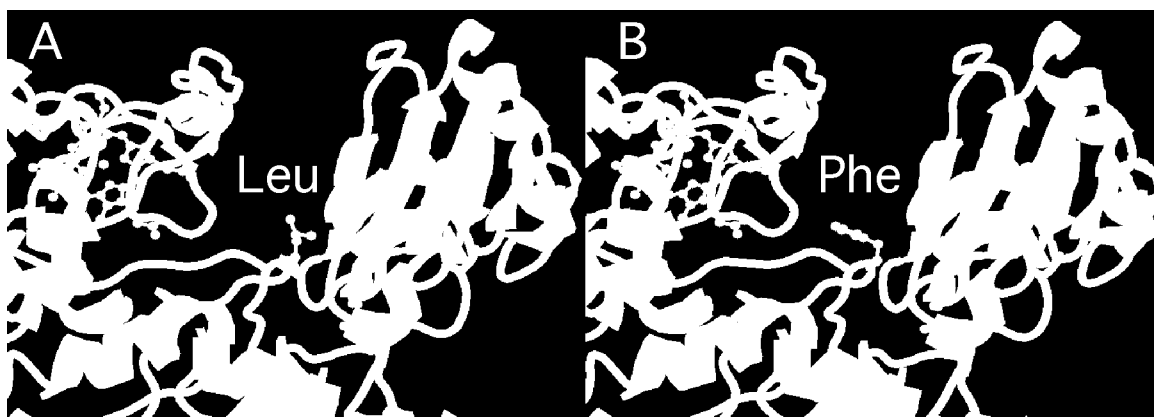


Figure 2. L286F mutation on the *ef* loop of the cyt *b* subunit of the *bc*₁ complex. The figure is to illustrate a hypothetical three-dimensional structure of the L286F mutant using the coordinates of the bovine heart mitochondrial *bc*₁ complex with the Fe-S subunit cluster domain in the intermediate position (5). Panels A and B depict the wild type L286 (corresponding to L262 in bovine numbering) and the mutant F286, respectively. Cyt *c*₁ with *c*₁ heme, cyt *b*, and the Fe-S subunit with its [2Fe2S] cluster are shown in different shades of gray. The amino acid at position 262 of cyt *b* corresponding to position 286 in *R. capsulatus* numbering is shown as stick and balls drawings, and one of its most favorable rotamer positions is chosen when it is substituted by a phenylalanine as shown in Panel B. The rotamer selection was carried out using the program Swiss-Pdb Viewer written by N. Guex and M. C. Peitsch (<http://www.pdb.bnl.gov/expasy/spdbv/mainpage.html>), and the coordinates visualized using Rasmol program written by R. Sayle (<http://www.umass.edu/microbio/rasmol/>).

Discussion

According to the structure of the *bc*₁ complex, the L286F mutation is located on the *ef* loop of cyt *b* that represents the most conspicuous barrier that needs to be crossed during the normal movement of the [2Fe2S] cluster domain from the Q_o site to the cyt *c*₁. Comparison of the structures with the cluster domain of the Fe-S subunit located at the intermediate position versus those where the Fe-S cluster domain is either in cyt *b* or cyt *c*₁ positions (5 and personal communication) indicates that the *ef* loop has moved away suggesting its flexibility. Previous observations that the movement of the Fe-S cluster domain is slowed down in the +1Ala mutant, and is even stopped when the hinge is longer (*i. e.*, +2Ala and +3Ala mutants) (14) are in good agreement with the motion of the cluster domain being hindered by the *ef* loop of cyt *b*. Moreover, the findings that the movement is prevented when the hinge is too rigid (*i. e.*, the 6Pro mutant where six amino acids are substituted by six proline residues in the hinge domain) but it could be restored when this rigid hinge is shortened to three proline residues (*i. e.*, 3ProΔ3) (15) also support this notion. In this respect, substituting the Leu286 (corresponding to Leu262 in bovine numbering) to a bulkier Phe residue may appear surprising to overcome a possible steric hindrance. However, it is noteworthy that the aromatic side chain of Phe is planar, and as illustrated in **Fig. 2** one of its most favorable rotamers could move this side chain away from the cluster domain of the Fe-S subunit. A more rigorous modeling of this suppression event should await the structure of the *bc*₁ complex from *R. capsulatus*, which is in progress (20).

Interestingly, the L286F mutation has mild disruptive effects on both the assembly of the Fe-S subunit and Q_o site catalysis, and it also lowers the E_m value of the [2Fe2S]

cluster both in the wild type and the mutant backgrounds. Thus it appears that the *ef* loop provides to the Q_o site its optimal catalytic properties when it has its native sequence. Previously, we had found that the soluble Fe-S subunit has a lower E_m value in comparison with its value when it is part of the *bc*₁ complex (17), and also in the presence of myxothiazol that tends to release the cluster domain from the stigmatellin-like position in the Q_o site (14). Thus conceivably, in the L286F mutant the cluster domain of the Fe-S subunit is now in a more polar environment. This change is apparently enough to counteract the tendency of holding the cluster domain deep into the Q_o site, to overcome the steric hindrance encountered and improve the Ps growth of the +1Ala/L286F double mutant. These findings therefore clearly illustrate the dual role played by the *ef* loop which apparently acts as a shield somehow protecting the Q_o site without constituting an insurmountable hindrance to the movement of the cluster domain of the Fe-S protein.

Acknowledgments

This work was supported by NIH grant GM 38237 to F. D.

References

1. Yu C-A Eds. (1999) *J. Bioenerg. Biomembr.* **31** (3), special issue on the cytochrome *bc*₁ complex.
2. Mitchell P. (1975) *FEBS Lett.*, **59**, 137-139.
3. Crofts AR, Meinhardt SW, Jones KR, Snozzi M (1983) *Biochim. Biophys. Acta* **723**, 202-218.
4. Zhang Z, Huang L, Shulmeister VM, Chi Y-I, Kim KK, Hung L-W, Crofts AR, Berry EA, Kim S-H (1998) *Nature* **392**, 677-684.
5. Iwata S, Lee JW, Okada K, Lee JK, Iwata M, Rasmussen B, Link TA, Ramaswamy S, Jap BK (1998) *Science* **281**, 64-71.
6. Hunte C, Koepke J, Lange C, Rossmannith T, Michel H (2000) *Structure* **8**, 669-684.
7. Kim H, Xia D, Yu C-A, Xia J-Z, Kachurin AM, Zhang L, Yu L, Deisenhofer J (1998) *Proc. Natl. Acad. Sci. USA* **95**, 8026-8033.
8. Tian H, Yu L, Mather MW, Yu C-A. (1998) *J. Biol. Chem.* **273**, 27953-27959.
9. Tian H., White, S., Yu, L., and Yu, C-A (1999) *J. Biol. Chem.* **274**, 7146-7152.
10. Xiao K, Yu L, Yu C-A (2000) *J. Biol. Chem.* **275**, 38597-38604.
11. Sadoski RC, Engstrom, G, Tian H, Zhang L, Yu C-A, Yu L, Durham B, Millett, F (2000) *Biochemistry* **39**, 4231-4236.
12. Nett JH, Hunte C, Trumpower BL (2000) *Eur. J. Biochem.* **267**, 5777-5782.
13. Brugna M, Rodgers S, Schricker A, Montoya G, Kazmeier M, Nitschke W, Sinning I (2000) *Proc. Natl. Acad. Sci. USA* **97**, 2069-2074.
14. Darrouzet E, Valkova-Valchanova M, Moser CC, Dutton PL, Daldal F (2000) *Proc. Natl. Acad. Sci. USA*. **97**, 4567-4572.
15. Darrouzet E, Valkova-Valchanova M, Daldal F (2000) *Biochemistry* **39**, 15475-15483.
16. Valkova-Valchanova M, Darrouzet E, Moomaw CR, Slaughter CA, Daldal F (2000) *Biochemistry*. **39**, 15484-15492.

17. Brasseur G, Sled V, Liebl U, Ohnishi T, Daldal F (1997) *Biochemistry* **36**, 11685-11696.
18. Atta-Asafo-Adjei E, Daldal F (1991) *Proc. Natl. Acad. Sci. USA* **88**, 492-496.
19. Saribas AS, Ding H, Dutton PL, Daldal F (1995) *Biochemistry* **34**, 16004-16012.
20. Berry, EA *et al.* Personal communication.